View metadata, citation and similar papers at core.ac.uk

brought to you by CORE

provided by Elsevier - Publisher Connector

Available online at www.sciencedirect.com

SCIENCE DIRECT®

Advances in Applied Mathematics 36 (2006) 106–117

ADVANCES IN Applied Mathematics

www.elsevier.com/locate/yaama

A geometric form for the extended patience sorting algorithm

Alexander Burstein [a,*], Isaiah Lankham [b,1]

[a] *Department of Mathematics, Iowa State University, Ames, IA 50011-2064, USA*
[b] *Department of Mathematics, University of California-Davis, Davis, CA 95616-8633, USA*

Received 1 June 2005; accepted 28 August 2005

Available online 15 December 2005

Abstract

Patience Sorting is a combinatorial algorithm that can be viewed as an iterated, non-recursive form of the Schensted Insertion Algorithm. In recent work the authors extended Patience Sorting to a full bijection between the symmetric group and certain pairs of combinatorial objects (called *pile configurations*) that are most naturally defined in terms of generalized permutation patterns and barred pattern avoidance. This Extended Patience Sorting Algorithm is very similar to the Robinson–Schensted–Knuth (or RSK) Correspondence, which is itself built from repeated application of the Schensted Insertion Algorithm.

In this work we introduce a geometric form for the Extended Patience Sorting Algorithm that is in some sense a natural dual algorithm to G. Viennot's celebrated Geometric RSK Algorithm. Unlike Geometric RSK, though, the lattice paths coming from Patience Sorting are allowed to intersect. We thus also give a characterization for the intersections of these lattice paths in terms of the pile configurations associated with a given permutation under the Extended Patience Sorting Algorithm.
© 2005 Elsevier Inc. All rights reserved.

MSC: 05A05; 05A18; 05E10

* Corresponding author.
E-mail addresses: burstein@math.iastate.edu (A. Burstein), issy@math.ucdavis.edu (I. Lankham).

[1] The work of the second author was supported in part by the US National Science Foundation under Grants DMS-0135345 and DMS-0304414.

0196-8858/$ – see front matter © 2005 Elsevier Inc. All rights reserved.
doi:10.1016/j.aam.2005.08.001

1. Introduction

The term *Patience Sorting* was introduced in 1962 by C.L. Mallows [8,9] as the name of a card sorting algorithm invented by A.S.C. Ross. This algorithm works by first partitioning a shuffled deck of n cards (which we take to be a permutation $\sigma \in \mathfrak{S}_n$) into sorted subsequences $r_1, r_2, \ldots, r_m$ called *piles* and then gathering the cards up in order from the tops of these piles. The procedure used in forming $r_1, r_2, \ldots, r_m$ can be viewed as an iterated, non-recursive form of the Schensted Insertion Algorithm for interposing values into the rows of a Young tableau (see [1,3]). Given $\sigma \in \mathfrak{S}_n$, we call this resulting collection of piles (given as part of the more general Algorithm 1.2 below) the *pile configuration* corresponding to σ and denote it by $R(\sigma)$.

Given a pile configuration R, one forms its *reverse patience word* $RPW(R)$ by listing the piles in R "from bottom to top, left to right" (i.e., by reversing the so-called "far-eastern reading") as illustrated in Example 1.1. In recent work [3] the authors used G. Viennot's (northeast) shadow diagram construction (defined in [12] and summarized in Section 2.1) to characterize these words in terms of the following pattern avoidance condition: Given $\sigma \in \mathfrak{S}_n$, each instance of the generalized permutation pattern 2-31 in $RPW(R(\sigma))$ must be contained within an instance of the pattern 3-1-42. We call this restricted form of the generalized permutation pattern 2-31 a (*generalized*) *barred permutation pattern* and denote it by 3-$\bar{1}$-42. This notational convention is due to J. West et al., and first appeared in the study of two-stack sortable permutations [5,6,13]. As usual, we denote the set of permutations $\sigma \in \mathfrak{S}_n$ that avoid the pattern 3-$\bar{1}$-42 by $S_n(3\text{-}\bar{1}\text{-}42)$. (See Bóna [2] for a review of permutation patterns in general.)

Example 1.1. Let $\sigma = 64518723 \in \mathfrak{S}_8$. Then, using a simplified form of Algorithm 1.2 below, σ has the pile configuration $R(\sigma) = \{\{6 > 4 > 1\}, \{5 > 2\}, \{8 > 7 > 3\}\}$, which is visually represented as the following array of numbers:

$$R(\sigma) \;=\; \begin{array}{ccc} 1 & & 3 \\ 4 & 2 & 7 \\ 6 & 5 & 8 \end{array}$$

Furthermore, $RPW(R(64518723)) = 64152873 \in S_8(3\text{-}\bar{1}\text{-}42)$.

In [3] the authors also extended the process of forming piles under Patience Sorting so that it essentially becomes a full non-recursive analog of the famous Robinson–Schensted–Knuth (or RSK) Correspondence. As with RSK, this Extended Patience Sorting Algorithm (Algorithm 1.2 below) takes a simple idea (that of placing cards into piles) and uses it to build a bijection between elements of the symmetric group $\mathfrak{S}_n$ and certain pairs of combinatorial objects. In the case of RSK, one uses the Schensted Insertion Algorithm to build a bijection with pairs of standard Young tableaux having the same shape (a partition λ of n, denoted $\lambda \vdash n$; see [10]). However, in the case of Patience Sorting, one achieves a bijection between permutations and somewhat more restricted pairs of pile configurations. In particular, these pairs must not only have the same shape (a composition γ of n, denoted $\gamma \circ\!\!- \; n$) but their reverse patience words must also simultaneously avoid containing certain generalized permutation patterns in the same positions (see [3] for more details). This restriction can also be understood geometrically using Viennot's (northeast) shadow diagram construction for the permutation implicitly defined by a pair of pile configurations (as is discussed in [3]), but a full geometric characterization requires the dual southwest shadow diagram construction used to define Geometric Patience Sorting in Section 3.

Viennot introduced the shadow diagram of a permutation in the context of studying the Schützenberger Symmetry Property for RSK (first proven using a direct combinatorial argument in [11]). Specifically, one can use recursively defined shadow diagrams to construct the RSK Correspondence completely geometrically via a sequence of recursively defined collections of non-intersecting lattice paths (with such collections called "shadow diagrams"). Then, using a particular labeling of the constituent "shadow lines" in each shadow diagram, one recovers successive rows in the usual RSK insertion and recording tableaux. The Schützenberger Symmetry Property for RSK then immediately follows since reflecting these shadow diagrams through the line "$y = x$" both inverts the permutation and exactly interchanges the labelings on the shadow lines that yield the rows in these tableaux.

We review Viennot's Geometric RSK Algorithm in Section 2 below. Then, in Section 3, we define a natural dual to Viennot's construction that similarly produces a geometric characterization of the Extended Patience Sorting Algorithm. As with RSK, the Schützenberger Symmetry Property is then immediate for Extended Patience Sorting. Unlike Geometric RSK, though, the lattice paths formed under Geometric Patience Sorting are allowed to intersect. Thus, having defined these two algorithms, we classify in Section 4 the types of intersections that can occur under Geometric Patience Sorting and then characterize when they occur in terms of the pile configurations associated to a given permutation under Extended Patience Sorting (Algorithm 1.2 below).

We close this introduction by stating the Extending Patience Sorting Algorithm and giving a complete example.

Algorithm 1.2 (*Extended Patience Sorting Algorithm*). Given a shuffled deck of cards $\sigma = c_1c_2\cdots c_n$, inductively build *insertion piles* $R = R(\sigma) = \{r_1, r_2, \ldots, r_m\}$ and *recording piles* $S = S(\sigma) = \{s_1, s_2, \ldots, s_m\}$ as follows:

- Place the first card c_1 from the deck into a pile r_1 by itself, and set $s_1 = \{1\}$.
- For each remaining card c_i $(i = 2, \ldots, n)$, consider the cards $d_1, d_2, \ldots, d_k$ atop the piles $r_1, r_2, \ldots, r_k$ that have already been formed.
  - If $c_i > \max\{d_1, d_2, \ldots, d_k\}$, then put c_i into a new pile r_{k+1} by itself and set $s_{k+1} = \{i\}$.
  - Otherwise, find the left-most card d_j that is larger than c_i and put the card c_i atop pile r_j while simultaneously putting i at the bottom of pile s_j.

Example 1.3. Let $\sigma = 64518723 \in \mathfrak{S}_8$. Then according to Algorithm 1.2 we simultaneously form the following pile configurations:

	insertion piles	recording piles		insertion piles	recording piles
Form a new pile with **6**:	**6**	**1**	Then play the **4** on it:	4 6	1 **2**
Form a new pile with **5**:	4 6 **5**	1 2 **3**	Add the **1** to left pile:	**1** 4 6 5	1 2 **4** 3

Form a	1			1			Then	1			1		
new pile	4			2			play the	4		**7**	2		5
with **8**:	6	5	**8**	4	3	**5**	**7** on it:	6	5	8	4	3	**6**
Add the **2**	1			1			Add the	1		**3**	1		5
to middle	4	**2**	7	2	3	5	**3** to right	4	2	7	2	3	6
pile:	6	5	8	4	**7**	6	pile:	6	5	8	4	7	**8**

The idea behind Algorithm 1.2 is that we are using a new pile configuration $S(\sigma)$ (called the "recording piles") to implicitly label the order in which the elements of the permutation σ are added to the usual Patience Sorting pile configuration $R(\sigma)$ (which we will now by analogy to RSK also call the "insertion piles"). It is clear that this information then allows us to uniquely reconstruct σ by reversing the order in which the cards were played. However, even though reversing the Extended Patience Sorting Algorithm is much easier than reversing the RSK Algorithm through recursive "reverse row bumping," the trade-off is that the pairs of pile configurations that result from the Extended Patience Sorting Algorithm are not independent (see [3] for more details), whereas the standard Young tableau pairs generated by RSK are completely independent (up to shape).

2. Northeast shadow diagrams and Viennot's geometric RSK

In this section we briefly develop Viennot's geometric form for RSK in order to motivate the geometric form for the Extended Patience Sorting that is introduced in Section 3 below.

2.1. The northeast shadow diagram of a permutation

We begin with the following fundamental definition:

Definition 2.1. Given a lattice point $(m, n) \in \mathbb{Z}^2$, we define the *northeast shadow* of (m, n) to be the quarter space $S_{NE}(m, n) = \{(x, y) \in \mathbb{R}^2 \mid x \geqslant m,\ y \geqslant n\}$.

See Figure 2.1(a) for an example of a point's northeast shadow.
The most important use of these shadows is in building so-called northeast shadowlines:

Definition 2.2. Given lattice points $(m_1, n_1), (m_2, n_2), \ldots, (m_k, n_k) \in \mathbb{Z}^2$, we define their *northeast shadowline* to be the boundary of the union of the northeast shadows $S_{NE}(m_1, n_1)$, $S_{NE}(m_2, n_2), \ldots, S_{NE}(m_k, n_k)$.

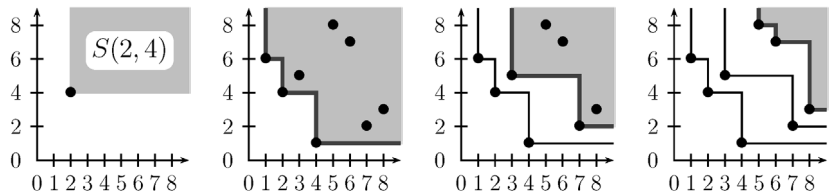

(a) The Shadow $S_{NE}(2, 4)$. (b) Shadowline $L_1(64518723)$. (c) Shadowline $L_2(64518723)$. (d) Shadowline $L_3(64518723)$.

Fig. 2.1. Examples of northeast shadow and shadowline constructions.

In particular, we wish to associate to each permutation a certain collection of northeast shadowlines (as illustrated in Figure 2.1(b)–(d)):

Definition 2.3. Given a permutation $\sigma = \sigma_1\sigma_2\cdots\sigma_n \in \mathfrak{S}_n$, the *northeast shadow diagram* $D^{(0)}_{NE}(\sigma)$ of σ consists of the shadowlines $L_1(\sigma), L_2(\sigma), \ldots, L_k(\sigma)$ formed as follows:

- $L_1(\sigma)$ is the northeast shadowline for the lattice points $\{(1,\sigma_1),(2,\sigma_2),\ldots,(n,\sigma_n)\}$.
- While at least one of the points $(1,\sigma_1),(2,\sigma_2),\ldots,(n,\sigma_n)$ is not contained in the shadowlines $L_1(\sigma), L_2(\sigma), \ldots, L_j(\sigma)$, define $L_{j+1}(\sigma)$ to be the northeast shadowline for the points

$$\left\{(i,\sigma_i) \;\middle|\; (i,\sigma_i) \notin \bigcup_{k=1}^{j} L_k(\sigma)\right\}.$$

In other words, we define the shadow diagram inductively by first taking $L_1(\sigma)$ to be the shadowline for the diagram $\{(1,\sigma_1),(2,\sigma_2),\ldots,(n,\sigma_n)\}$ of the permutation. Then we ignore the lattice points whose shadows were used in building $L_1(\sigma)$ and define $L_2(\sigma)$ to be the shadowline of the resulting subset of the permutation diagram. We then build $L_3(\sigma)$ as the shadowline for the points not yet used in constructing either $L_1(\sigma)$ or $L_2(\sigma)$, and this process continues until all points in the permutation diagram are exhausted.

We can characterize the points whose shadows define the shadowlines at each stage as follows: they are the smallest collection of unused points whose shadows collectively contain all other remaining unused points (and hence also contain the shadows of those points). As a consequence of this shadow containment property, the shadowlines in a northeast shadow diagram will never cross. However, as we will see in Section 3.1 below, the dual construction to Definition 2.3 that is introduced will allow for crossing shadowlines, which are then classified and characterized in Section 4. The most fundamental cause for this distinction is the way that we will reverse the above shadow containment property for the points used in defining southwest shadowlines.

2.2. Viennot's geometric RSK algorithm

As simple as northeast shadowlines were to define in the previous section, a great deal of information can still be gotten from them. One of the most basic properties of the northeast shadow diagram $D^{(0)}_{NE}(\sigma)$ for a permutation $\sigma \in \mathfrak{S}_n$ is that it encodes the top row of the RSK insertion tableau $P(\sigma)$ (respectively recording tableau $Q(\sigma)$) as the smallest ordinates (respectively smallest abscissae) of all points belonging to the constituent shadowlines $L_1(\sigma), L_2(\sigma), \ldots, L_k(\sigma)$. One proves this by comparing the use of Schensted Insertion on the top row of the insertion tableau with the intersection of vertical lines having the form $x = a$. In particular, as a increases from 0 to n, the line $x = a$ intersects the lattice points in the permutation diagram in the order that they are inserted into the top row, and so shadowlines connect elements of σ to those smaller elements that will eventually bump them. (See Sagan [10] for more details.)

Remarkably, one can then use the northeast corners (called the *salient points*) of $D^{(0)}_{NE}(\sigma)$ to form a new shadow diagram $D^{(1)}_{NE}(\sigma)$ that similarly gives the second rows of $P(\sigma)$ and $Q(\sigma)$. Then, inductively, the salient points of $D^{(1)}_{NE}(\sigma)$ can be used to give the third rows of $P(\sigma)$ and $Q(\sigma)$, and so on. As such, one can view this recursive formation of shadow diagrams as a geometric form for the RSK correspondence. We illustrate this process in Fig. 2.2 for the following permutation from Example 1.3:

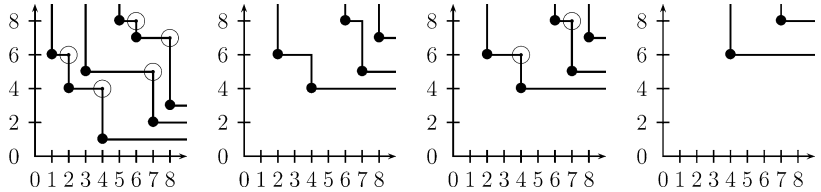

(a) Salient points for $D^{(0)}_{NE}(64518723)$. (b) Shadow Diagram $D^{(1)}_{NE}(64518723)$. (c) Salient points for $D^{(1)}_{NE}(64518723)$. (d) Shadow Diagram $D^{(2)}_{NE}(64518723)$.

Fig. 2.2. The northeast shadow diagrams for the permutation $64518723 \in \mathfrak{S}_8$.

$$\sigma = 64518723 \overset{RSK}{\longleftrightarrow} \left(\begin{array}{|c|c|c|}\hline 1&2&3\\\hline 4&5&7\\\hline 6&8\\\cline{1-2} \end{array}\ , \begin{array}{|c|c|c|}\hline 1&3&5\\\hline 2&6&8\\\hline 4&7\\\cline{1-2} \end{array} \right).$$

3. Southwest shadow diagrams and geometric patience sorting

In this section we introduce a very natural dual algorithm to Viennot's geometric form for RSK as given in Section 2.2.

3.1. The southwest shadow diagram of a permutation

As in Section 2.1, we begin with the following fundamental definition:

Definition 3.1. Given a lattice point $(m, n) \in \mathbb{Z}^2$, we define the *southwest shadow* of (m, n) to be the quarter space $S_{SW}(m, n) = \{(x, y) \in \mathbb{R}^2 \mid x \leqslant m,\ y \leqslant n\}$.

See Fig. 3.1(a) for an example of a point's southwest shadow.

As with their northeast counterparts, the most important use of these shadows is in building southwest shadowlines:

Definition 3.2. Given lattice points $(m_1, n_1), (m_2, n_2), \ldots, (m_k, n_k) \in \mathbb{Z}^2$, we define their *southwest shadowline* to be the boundary of the union of the shadows $S_{SW}(m_1, n_1)$, $S_{SW}(m_2, n_2), \ldots, S_{SW}(m_k, n_k)$.

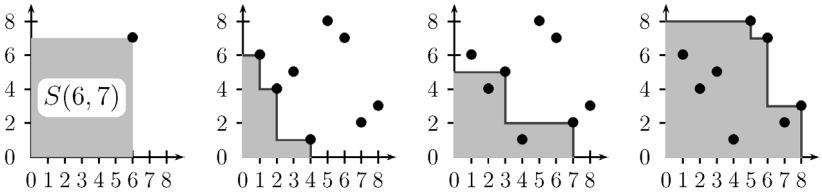

(a) The Shadow $S_{SW}(6, 7)$. (b) Shadowline $L^{(0)}_1(64518723)$. (c) Shadowline $L^{(0)}_2(64518723)$. (d) Shadowline $L^{(0)}_3(64518723)$.

Fig. 3.1. Examples of southwest shadow and shadowline constructions.

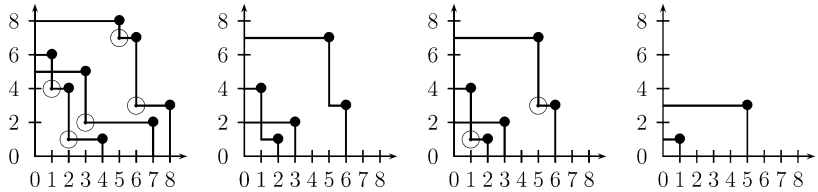

(a) Salient points for $D_{SW}^{(0)}(64518723)$. (b) Shadow Diagram $D_{SW}^{(1)}(64518723)$. (c) Salient points for $D_{SW}^{(1)}(64518723)$. (d) Shadow Diagram $D_{SW}^{(2)}(64518723)$.

Fig. 3.2. The southwest shadow diagrams for the permutation $64518723 \in \mathfrak{S}_8$.

In particular, we wish to associate to each permutation a certain collection of southwest shadowlines. However, unlike the northeast case, these shadowlines sometimes cross (as illustrated in Figs. 3.1(b)–(d) and Fig. 3.2(a)).

Definition 3.3. Given a permutation $\sigma = \sigma_1\sigma_2\cdots\sigma_n \in \mathfrak{S}_n$, the *southwest shadow diagram* $D_{SW}^{(0)}(\sigma)$ of σ consists of the southwest shadowlines $L_1^{(0)}(\sigma), L_2^{(0)}(\sigma), \ldots, L_k^{(0)}(\sigma)$ formed as follows:

- $L_1^{(0)}(\sigma)$ is the shadowline for those lattice points $(x, y) \in \{(1, \sigma_1), (2, \sigma_2), \ldots, (n, \sigma_n)\}$ such that $S_{SW}(x, y)$ does not contain any other lattice point.
- While at least one of the points $(1, \sigma_1), (2, \sigma_2), \ldots, (n, \sigma_n)$ is not contained in the shadowlines $L_1^{(0)}(\sigma), L_2^{(0)}(\sigma), \ldots, L_j^{(0)}(\sigma)$, define $L_{j+1}^{(0)}(\sigma)$ to be the shadowline for the points

$$(x, y) \in \left\{ (i, \sigma_i) \;\middle|\; (i, \sigma_i) \notin \bigcup_{k=1}^{j} L_k^{(0)}(\sigma) \right\}$$

such that $S_{SW}(x, y)$ does not contain any other lattice point in the same set.

In other words, we again define a shadow diagram by recursively eliminating certain points in the permutation diagram until every point has been used to define a shadowline. However, we are here reversing both the direction of the shadows and the shadow containment property from the northeast case. It is in this sense that the geometric form for the Extended Patience Sorting Algorithm given in the next section can be viewed as "dual" to Viennot's geometric form for RSK.

3.2. The geometric patience sorting algorithm

As in Section 2.2, one can produce a sequence $D_{SW}(\sigma) = (D_{SW}^{(0)}(\sigma), D_{SW}^{(1)}(\sigma), D_{SW}^{(2)}(\sigma), \ldots)$ of shadow diagrams for a given permutation $\sigma \in \mathfrak{S}_n$ by recursively applying Definition 3.3 to salient points, with the restriction that new shadowlines can only connect points that were on the same shadowline in the previous iteration. (The reason for this important distinction from Geometric RSK is discussed further in Section 4.1.) The salient points in this case are then naturally defined to be the southwest corner points of a given set of shadowlines. See Fig. 3.2 for an example of how this works for the permutation from Example 1.3.

Definition 3.4. We call $D_{SW}^{(k)}(\sigma)$ the kth *iterate* of the *exhaustive shadow diagram* $D_{SW}(\sigma)$ for $\sigma \in \mathfrak{S}_n$.

Moreover, the resulting sequence of shadow diagrams can then be used to reconstruct the pair of pile configurations given by the Extended Patience Sorting Algorithm (Algorithm 1.2). To accomplish this, index the cards in a pile configuration using the French convention for tableaux so that the row index increases from bottom to top and the column index from left to right. (In other words, we are labeling boxes as we would lattice points in the first quadrant of $\mathbb{R}^2$.) Then, for a given permutation $\sigma \in \mathfrak{S}_n$, the elements of the ith row of the insertion piles $R(\sigma)$ (respectively recording piles $S(\sigma)$) are given by the largest ordinates (respectively abscissae) of the shadowlines that compose $D_{SW}^{(i)}$.

The main difference between this process and Viennot's Geometric RSK is that care must be taken to assemble each row in its proper order. Unlike the entries of a Young tableau, the elements in the rows of a pile configuration do not necessarily increase from left to right, and they do not have to be contiguous. As such, the components of each row should be recorded in the order that the shadowlines are formed. The rows can then uniquely be assembled into a legal pile configuration since the elements in the columns of a pile configuration must both decrease (when read from bottom to top) and appear in the leftmost pile possible.

The proof of this is along the same lines as that of Viennot's Geometric RSK in that the shadowlines produced by Definition 3.3 are a visual record for how cards are played atop each other under Algorithm 1.2. In particular, it should be clear that, given a permutation $\sigma \in \mathfrak{S}_n$, the shadowlines in both of the shadow diagrams $D_{SW}^{(0)}(\sigma)$ and $D_{NE}^{(0)}(\sigma)$ are defined by the same lattice points from the permutation diagram for σ. In [3] the points along a given northeast shadowline are shown to correspond exactly to the elements in some column of $R(\sigma)$ (as both correspond to one of the left-to-right minima subsequences of σ). Thus, by reading the lattice points in the permutation diagram in increasing order of their abscissae, one can uniquely reconstruct both the piles in $R(\sigma)$ and the exact order in which cards are added to these piles (which implicitly yields $S(\sigma)$). In this sense, both $D_{SW}^{(0)}(\sigma)$ and $D_{NE}^{(0)}(\sigma)$ encode the bottom rows of $R(\sigma)$ and $S(\sigma)$ as given by Algorithm 1.2.

It is then easy to see by induction that the salient points of $D_{SW}^{(k-1)}(\sigma)$ yield the kth rows of $R(\sigma)$ and $S(\sigma)$, and so this gives the following

Theorem 3.5. *The process described above for creating a pair of pile configurations* $(R'(\sigma), S'(\sigma))$ *from the Geometric Patience Sorting construction yields the same pair of pile configurations* $(R(\sigma), S(\sigma))$ *as the Extended Patience Sorting Algorithm* (*Algorithm* 1.2).

Having given the above Geometric form for Algorithm 1.2, it is worth pointing out that—as with RSK—there are various natural generalizations of Extended Patience Sorting for more general combinatorial objects including words and lexicographic arrays. (See [7] for a description of such extensions of RSK.) Moreover, many of these generalizations can still similarly be realized as non-recursive analogs for the forms of RSK that can be applied to such objects. In particular, the authors in [4] explore several such generalizations and develop geometric forms for them much like the one given in this section.

In the case of words, Aldous and Diaconis [1] have given two different generalizations for Patience Sorting based upon whether cards with equal value are played on top of each other or not. These are called the "ties allowed" and "ties forbidden" cases, respectively, and the usual

RSK and dual RSK algorithms can be modeled in order to develop bijective versions of them. The geometric forms for the resulting algorithms as given in [4] can then be compared to Fulton's "Matrix-Ball" Geometric RSK algorithm (defined in [7]) just as we compare the Geometric Patience Sorting given in this section to Viennot's Geometric RSK in Section 4.

4. Geometric patience sorting and intersecting lattice paths

Extended Patience Sorting (Algorithm 1.2) can be viewed as a "non-bumping" version of the RSK algorithm for permutations in that cards are permanently placed into piles and are covered by other cards rather being displaced by them. It is in this sense that one of the main differences between their geometric algorithms lies in how and in what order (when read from left to right) the salient points of their respective shadow diagrams are determined. In particular, as playing a card atop a pre-existing pile under Patience Sorting is essentially like non-recursive Schensted Insertion, certain particularly egregious "multiple bumps" that occur under the Schensted Insertion Algorithm prove to be too complicated to be properly modeled by the "static insertions" of Patience Sorting.

At the same time, it is also easy to see that for a given $\sigma \in \mathfrak{S}_n$, the cards atop the piles in the pile configurations $R(\sigma)$ and $S(\sigma)$ (as given by Algorithm 1.2) are exactly the cards in the top rows of the RSK insertion tableau $P(\sigma)$ and recording tableau $Q(\sigma)$, respectively. Thus, this raises the question of when the remaining rows of $P(\sigma)$ and $Q(\sigma)$ can likewise be recovered from $R(\sigma)$ and $S(\sigma)$. While this appears to be directly related to the order in which salient points are read (as illustrated in Example 4.1 below), one would ultimately hope to characterize the answer in terms of generalized pattern avoidance similar to the description of reverse patience words for pile configurations (as given in [3]).

Example 4.1. Consider the northeast and southwest shadow diagrams for $\sigma = 2431$:

$D^{(0)}_{NE}(2431) =$ 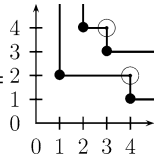 vs. $D^{(0)}_{SW}(2431) =$ 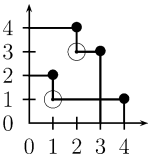

In particular, note that the order in which the salient points are formed (when read from left to right) is reversed. Such reversals serve to illustrate one of the inherent philosophical differences between RSK and the Extended Patience Sorting Algorithm.

As mentioned in Section 3.2, another fundamental difference between Geometric RSK and Geometric Patience Sorting is that the latter allows certain crossings to occur in the lattice paths formed during the same iteration of the algorithm. We classify these crossings in Section 4.1 and then characterize those permutations that yield entirely non-intersecting lattice paths in Section 4.2.

4.1. Types of crossings in geometric patience sorting

Given $\sigma \in \mathfrak{S}_n$, we can classify the basic types of crossings in $D^{(0)}_{SW}(\sigma)$ as follows: First note that each southwest shadowline in $D^{(0)}_{SW}(\sigma)$ corresponds to a pair of decreasing sequences of the same length, namely a column from the insertion piles $R(\sigma)$ and its corresponding column from

the recording piles $S(\sigma)$. Then, given two different pairs of such columns in $R(\sigma)$ and $S(\sigma)$, the shadowline corresponding to the rightmost (respectively leftmost) pair—under the convention that new columns are always added to the right of all other columns in Algorithm 1.2)—is called the *upper* (respectively *lower*) shadowline. More formally:

Definition 4.2. Given two shadowlines, $L_i^{(m)}(\sigma), L_j^{(m)}(\sigma) \in D_{SW}^{(m)}(\sigma)$ with $i < j$, we call $L_i^{(m)}(\sigma)$ the *lower* shadowline and $L_j^{(m)}(\sigma)$, the *upper* shadowline. Moreover, if $L_i^{(m)}(\sigma)$ and $L_j^{(m)}(\sigma)$ intersect, then we call this a *vertical crossing* (respectively *horizontal crossing*) if it involves a vertical (respectively horizontal) segment of $L_j^{(m)}(\sigma)$.

We illustrate these crossings in the following example. In particular, note that the only permutations $\sigma \in \mathfrak{S}_3$ of length three having intersections in their 0th iterate shadow diagram $D_{SW}^{(0)}(\sigma)$ are $312, 231 \in \mathfrak{S}_3$.

Example 4.3.

(1) The smallest permutation for which $D_{SW}^{(0)}(\sigma)$ contains a horizontal crossing is $\sigma = 312$ as illustrated in Fig. 4.1(a). The upper shadowline involved in this crossing is the one with only two segments.
(2) The smallest permutation for which $D_{SW}^{(0)}(\sigma)$ contains a vertical crossing is $\sigma = 231$ as illustrated in Fig. 4.1(b). As in part (1), the upper shadowline involved in this crossing is again the one with only two segments.
(3) Consider $\sigma = 4231$. From Fig. 4.1(c), $D_{SW}^{(0)}(\sigma)$ contains exactly two southwest shadowlines, and these shadowlines form a horizontal crossing followed by a vertical crossing. We call a configuration like this a "polygonal crossing." Note in particular that $D_{SW}^{(1)}(\sigma)$ (trivially) has no crossings.
(4) Consider $\sigma = 45312$. From Fig. 4.1(d), $D_{SW}^{(0)}(\sigma)$ not only has a "polygonal crossing" (this time as two shadowlines have a vertical crossing followed by a horizontal one) but $D_{SW}^{(1)}(\sigma)$ does as well.

Polygonal crossings are what make it necessary to read only the salient points along the same shadowline in the order in which shadowlines are formed (as opposed to constructing the subsequent shadowlines using the entire partial permutation of salient points as in Viennot's Geometric RSK).

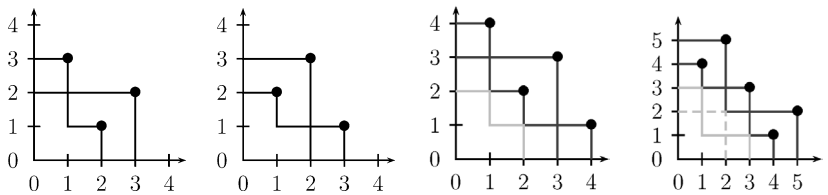

(a) Shadow Diagram $D_{SW}^{(0)}(312)$. (b) Shadow Diagram $D_{SW}^{(0)}(231)$. (c) Shadow Diagrams $D_{SW}^{(0)}, D_{SW}^{(1)}(4231)$. (d) Shadow Diagrams $D_{SW}^{(0)}, D_{SW}^{(1)}(45312)$.

Fig. 4.1. Shadow diagrams with different types of crossings.

Example 4.4. Consider the shadow diagram of $\sigma = 45312$ as illustrated in Fig. 4.1(d). The 0th iterate shadow diagram $D_{SW}^{(0)}$ contain a polygonal crossing, and so the 1st iterate shadow diagram $D_{SW}^{(1)}$ needs to be formed as indicated in order to properly describe the pile configurations $R(\sigma)$ and $S(\sigma)$ since

$$\sigma = 45312 \overset{XPS}{\longleftrightarrow} \begin{pmatrix} 1 & & 1 & \\ 3 & 2 & 3 & 2 \\ 4 & 5, & 4 & 5 \end{pmatrix} \tag{1}$$

under the Extended Patience Sorting Algorithm.

4.2. Non-intersecting shadow diagrams

Unlike the rows of Young tableaux, the values in the rows of a pile configuration do not necessarily increase when read from left to right. In fact, the descents in the rows of pile configurations are very closely related to the crossings given by Geometric Patience Sorting.

As noted in Section 3.2, Geometric Patience Sorting is ostensibly simpler than Geometric RSK in that one can essentially recover both the insertion piles $R(\sigma)$ and the recording piles $S(\sigma)$ from the 0th iterate shadow diagram $D_{SW}^{(0)}$. The fundamental use, then, of the iterates $D_{SW}^{(i+1)}, D_{SW}^{(i+2)}, \ldots$ is in understanding the intersections in the ith iterate shadow diagram $D_{SW}^{(i)}$. In particular, each shadowline $L_i^{(m)}(\sigma) \in D_{SW}^{(m)}(\sigma)$ corresponds to the pair of segments of the ith columns of $R(\sigma)$ and $S(\sigma)$ that are above the mth row (or are the ith columns if $m = 0$), where rows are numbered from bottom to top.

Theorem 4.5. *Each iterate $D_{SW}^{(m)}(\sigma)$ $(m \geqslant 0)$ of $\sigma \in \mathfrak{S}_n$ is free from crossings if and only if every row in both $R(\sigma)$ and $S(\sigma)$ is monotone increasing from left to right.*

Proof. Since each $L_i^{(m)} = L_i^{(m)}(\sigma)$ depends only on the ith columns of $R = R(\sigma)$ and $S = S(\sigma)$ above row m, we may assume without loss of generality that R and S have the same shape with exactly two columns.

Let $m+1$ be the highest row where a descent occurs in either R or S. If this descent occurs in R, then $L_2^{(m)}$ is the upper shadowline in a horizontal crossing since $L_2^{(m)}$ has y-intercept below that of $L_1^{(m)}$, which is the lower shadowline in this crossing (as in 312). If this descent occurs in S, then $L_2^{(m)}$ is the upper shadowline in a vertical crossing since $L_2^{(m)}$ has x-intercept to the left of $L_1^{(m)}$, which is the lower shadowline in this crossing (as in 231). Note that both descents may occur simultaneously (as in 4231 or 45312).

Conversely, suppose m is the last iterate at which a crossing occurs in $D_{SW}(\sigma)$ (i.e., $D_{SW}^{(\ell)}(\sigma)$ has no crossings for $\ell > m$). We will prove that $L_2^{(m)}$ may have a crossing only at the first or last segment. This, in turn, implies that row m in R or S is decreasing. A crossing occurs when there is a vertex of $L_1^{(m)}$ not in the shadow of any point of $L_2^{(m)}$. We will prove that it can only be the first or last vertex. Let $\{(s_1, r_1), (s_2, r_2), \ldots\}$ and $\{(u_1, t_1), (u_2, t_2), \ldots\}$ be the vertices that define $L_1^{(m)}$ and $L_2^{(m)}$, respectively. Then $\{r_i\}_{i \geqslant 1}$ and $\{t_i\}_{i \geqslant 1}$ are decreasing while $\{s_i\}_{i \geqslant 1}$ and $\{u_i\}_{i \geqslant 1}$ are increasing. Write $(a, b) \leqslant (c, d)$ if (a, b) is in the shadow of (c, d) (i.e. if $a \leqslant b$ and $c \leqslant d$), and consider $L_1^{(m+1)}$ and $L_2^{(m+1)}$. They are noncrossing

and defined by points $\{(s_1, r_2), (s_2, r_3), \ldots\}$ and $\{(u_1, t_2), (u_2, t_3), \ldots\}$, respectively. Then, for any i, $(s_i, r_{i+1}) \leqslant (u_j, t_{j+1})$ for some j. Suppose $(s_i, r_{i+1}) \leqslant (u_j, t_{j+1})$ and $(s_{i+1}, r_{i+2}) \leqslant (u_k, t_{k+1})$ for some $j < k$. Each upper shadowline vertex must contain some lower shadowline vertex in its shadow, so for all $\ell \in [j, k]$, $(s_i, r_{i+1}) \leqslant (u_\ell, t_{\ell+1})$ or $(s_{i+1}, r_{i+2}) \leqslant (u_\ell, t_{\ell+1})$. Choose the least $\ell \in [j, k]$ such that $(s_{i+1}, r_{i+2}) \leqslant (u_\ell, t_{\ell+1})$. If $(s_i, r_{i+1}) \leqslant (u_\ell, t_{\ell+1})$, then $(s_{i+1}, r_{i+1}) \leqslant (u_\ell, t_{\ell+1}) \leqslant (u_\ell, t_\ell)$. If $(s_i, r_{i+1}) \not\leqslant (u_\ell, t_{\ell+1})$, then $(s_i, r_{i+1}) \leqslant (u_{\ell-1}, t_\ell)$, so $(s_{i+1}, r_{i+1}) \leqslant (u_\ell, t_\ell)$. Thus, in both cases, $(s_{i+1}, r_{i+1}) \leqslant (u_\ell, t_\ell)$, and the desired conclusion follows.

An immediate corollary of the above proof is that all rows $i \geqslant m$ in both $R(\sigma)$ and $S(\sigma)$ are monotone increasing from left to right if and only if every iterate $D_{SW}^{(i)}(\sigma)$ $(i \geqslant m)$ is free from crossings.

One can equivalently characterize intersecting shadowlines beyond the 0th iterate of $\sigma \in \mathfrak{S}_n$ in terms of sub-pile patterns for the entries in $R(\sigma)$ and $S(\sigma)$. We state the following such result only for horizontal crossings, but vertical crossings can then be characterized by inverting σ (i.e., by transposing within these pairs of patterns via a Schützenberger-type symmetry result proven in [3]). Moreover, it is not difficult to show that avoiding both horizontal and vertical crossings in every iterate is equivalent to avoiding all crossings.

Corollary 4.6. *If $R(\sigma)$ and $S(\sigma)$ contain either of the following two simultaneous sub-pile patterns, then the permutation $\sigma \in \mathfrak{S}_n$ has a horizontal crossing in $D_{SW}^{(m)}(\sigma)$ (here $\{x_s\}_{s \geqslant 1}$ and $\{y_r\}_{r \geqslant 1}$ are monotone increasing; $m \leqslant k, l$; and the numbers in the boxes indicate the number of elements in respective sub-piles)*:

$$\begin{array}{ll} \boxed{i} & \\ y_1 \quad \boxed{j} & \\ y_3 \quad y_2 & \\ \boxed{k} \quad \boxed{m} & \end{array} \subset R, \quad \begin{array}{lll} \boxed{k-m} & & \\ x_1 & & \boxed{0} \\ x_2 & & x_3 \\ \boxed{i+m} & & \boxed{j+m} \end{array} \subset S \quad \text{or} \quad \begin{array}{ll} \boxed{i} & \\ y_1 \quad \boxed{j} & \\ y_3 \quad y_2 & \\ \boxed{k} \quad \boxed{l} & \end{array} \subset R, \quad \begin{array}{ll} \boxed{k-m} & \boxed{l-m} \\ x_2 & x_1 \\ x_3 & x_4 \\ \boxed{i+m} & \boxed{j+m} \end{array} \subset S.$$

References

[1] D. Aldous, P. Diaconis, Longest increasing subsequences: From patience sorting to the Baik–Deift–Johansson theorem, Bull. Amer. Math. Soc. 36 (1999) 413–432, available online at http://www.ams.org/bull/1999-36-04/.
[2] M. Bóna, Combinatorics of Permutations, Chapman & Hall/CRC Press, 2004.
[3] A. Burstein, I. Lankham, Combinatorics of patience sorting piles, in: Proceedings of Formal Power Series and Algebraic Combinatorics (FPSAC 2005), June 2005, Taormina, Italy.
[4] A. Burstein, I. Lankham, Patience sorting on words and lexicographic arrays, in preparation.
[5] S. Dulucq, S. Gire, O. Guibert, A combinatorial proof of J. West's conjecture, Discrete Math. 187 (1998) 71–96.
[6] S. Dulucq, S. Gire, J. West, Permutations with forbidden subsequences and nonseparable maps, Discrete Math. 153 (1996) 85–103.
[7] W. Fulton, Young Tableaux, London Math. Soc. Stud. Texts, vol. 35, Cambridge Univ. Press, 1997.
[8] C.L. Mallows, Problem 62-2, patience sorting, SIAM Rev. 4 (1962) 148–149.
[9] C.L. Mallows, Problem 62-2, SIAM Rev. 5 (1963) 375–376.
[10] B. Sagan, The symmetric group, second ed., in: Grad. Texts in Math., vol. 203, Springer, 2000.
[11] M.P. Schützenberger, Quelques remarques sur une construction de Schensted, Math. Scand. 12 (1963) 117–128.
[12] G. Viennot, Une forme géométrique de la correspondance de Robinson–Schensted, in: D. Foata (Ed.), Combinatoire et Représenatation du Groupe Symétrique, in: Lecture Notes in Math., vol. 579, Springer, 1977, pp. 29–58.
[13] J. West, Permutations with forbidden subsequences and stack-sortable permutations, PhD thesis, MIT, 1990.